

RESEARCH

Open Access



# Potential toxicity of micro- and nanoplastics in primary bronchial epithelial cells of patients with chronic obstructive pulmonary disease

I. F. Gosselink<sup>1</sup>, P. Leonhardt<sup>1</sup>, M. J. Drittij<sup>1</sup>, E. Weltjens<sup>1</sup>, P. J. J. Jessen<sup>1</sup>, F. G. A. J. van Belleghem<sup>3,4</sup>, K. Smeets<sup>3</sup>, I. M. Kooter<sup>1,2,4</sup>, F. J. van Schooten<sup>1</sup> and Alexander H. V. Remels<sup>1\*</sup>

## Abstract

**Background** The environmental presence of airborne micro- and nanoplastics (MNPs) raises concerns about their impact on the development and progression of respiratory diseases, including chronic obstructive pulmonary disease (COPD). In this study, we investigated the potential toxicity of amorphous, environmentally relevant MNPs in primary bronchial epithelial cells (PBEC) exposed at the air-liquid interface (ALI).

**Methods** Differentiated PBEC cultures from COPD donors ( $n=3$ ) and non-COPD donors ( $n=3$ ) were exposed for 24 h to polyvinylchloride (PVC), polypropylene (PP), or polyamide-6,6 (PA) MNPs ( $>75\%$  of particles  $<1\text{ }\mu\text{m}$ ) via small droplet application. Cytotoxicity, inflammation, cellular composition, morphology and integrity of the epithelial barrier as well as antioxidant and autophagy-related processes were assessed by a combination of lactate dehydrogenase leakage, IL-8 secretion, transmission electron microscopy and gene expression analyses.

**Results** All PBEC cultures formed an intact epithelial barrier. However, transepithelial electrical resistance (TEER) and transcript levels of tight junction protein Claudin 4 were lower ( $FC=0.36$ ,  $p=0.02$ ) in COPD-PBEC versus non-COPD PBEC. Although with some inter-donor variability, MNPs did not induce profound cytotoxicity or inflammation. However, PA MNPs ( $3\text{ }\mu\text{g}/\text{cm}^2$ ), decreased expression of Zonula Occludens-1 ( $FC=0.76$ ,  $p=0.01$ ), Occludin ( $FC=0.75$ ,  $p=0.03$ ) and modulated cell-type specific genes in COPD-PBEC, suggesting (early) epithelial barrier disruption. Additionally, differential regulation of transcript levels of antioxidant, apoptotic and autophagy genes was observed between COPD and non-COPD in response to PVC and PA.

**Conclusion** These results indicate that MNP exposure, especially PA, can induce (sub)toxic effects in PBEC, with substantial inter-donor variability. Whether this impacts COPD development remains to be studied.

**Keywords** Nanoplastics, Polypropylene, Polyamide, Polyvinylchloride, COPD

<sup>1</sup>Deceased: I. M. Kooter.

\*Correspondence:

Alexander H. V. Remels  
a.remels@maastrichtuniversity.nl

<sup>1</sup>Institute of Nutrition and Translational Research in Metabolism (NUTRIM),  
Department of Pharmacology and Toxicology, Maastricht University,  
Universiteitssingel 50, Maastricht 6229 ER, The Netherlands

<sup>2</sup>Netherlands Organization for Applied Scientific Research, TNO,  
Utrecht 3584 CB, The Netherlands

<sup>3</sup>Research Group Zoology: Biodiversity & Toxicology, Centre for  
Environmental Sciences, Hasselt University, Diepenbeek 3590, Belgium

<sup>4</sup>Department of Environmental Sciences, Faculty of Science, Open  
Universiteit, Heerlen 6419 AT, The Netherlands

*In memory of I. Kooter.*

## Introduction

According to the World Health Organization, 99% of all people worldwide are breathing air that exceeds air-quality limits [1]. In the last years, microplastics ( $> 1 \mu\text{m}$ ) and nanoplastics ( $< 1 \mu\text{m}$ ) (MNPs) have been increasingly recognized as emerging pollutants of concern and have been detected in both indoor and outdoor air [2]. Individual nanoplasic exposure via inhalation is highly variable, and difficult to measure due to technical limitations. Estimated microplastic exposures via air are  $1.07 \times 10^{-7}$  mg/capita/day, and can increase significantly in occupational settings [3, 4].

Airborne MNPs can derive from various sources, including synthetic textiles, housing furniture and tire wear [5]. Due to their small size, MNPs can be inhaled and deposited in both the upper airways as well as deeper areas of the lung [6]. Evidencing exposure via the inhalation route, MNPs of several polymers, including polyvinylchloride (PVC), polyamide (PA), and polypropylene (PP) have been detected in all areas of the lung as well as in sputum and bronchoalveolar lavage fluid (BALF) [7–9]. In addition, it has been established that MNPs can cross the bronchial- and alveolar epithelial barrier, and translocate to other organs [10, 11]. Despite this, the impact of MNPs on human health, specifically on the respiratory epithelium, remains to be determined.

Air pollution in general is considered a major risk factor for the development and progression of respiratory diseases, including chronic obstructive pulmonary disease (COPD). COPD is a chronic and irreversible lung disease that is characterized by progressive airflow limitation, tissue destruction and remodeling of both the alveolar- and bronchial epithelium. More than 200 million cases are diagnosed per year across the globe [12]. Although correlations have been suggested between MNPs exposure and lung cancer, whether or not there is a link between COPD and MNPs remains to be determined [13, 14]. Initial evidence has however detected an increased amount of microplastics in the sputum of COPD patients, compared to non-COPD patients [15]. Due to technical limitations, this study was unable to detect nanoplastics.

The bronchial epithelium is the first barrier encountered by inhaled particles and is crucial in preventing the trespassing and clearance of these substances. Multiple studies have demonstrated that both the functionality as well as the cellular composition of the bronchial epithelial barrier is impaired in COPD patients [16–18]. COPD patients, for example, display decreased cilia function, goblet cell hyperplasia and a decreased barrier integrity resulting from impairments in tight junctions [18–20]. Multiple cellular processes contribute to these pathological changes in the bronchial epithelial layer in COPD.

These include changes in redox status, the presence of (chronic) inflammation and activation of processes such as apoptosis and autophagy [21, 22]. Intriguingly, studies have demonstrated that MNPs can induce inflammation, oxidative stress and activate autophagy pathways in bronchial epithelial cells, hinting at a potential link between MNP exposure and COPD pathogenesis [23]. For example, acute airborne polystyrene (PS) nanoparticle exposure induced cytokine levels, among which interleukin-6 (IL-6) and Tumor Necrosis Factor Alpha (TNF- $\alpha$ ), in BALF, lung tissue and serum in mice. The same study observed increased reactive oxygen species (ROS) levels, tissue hyperplasia and induced inflammatory cell infiltration in mice exposed to PS nanoparticles [24]. In addition, PA nanoplasic exposure induced cytotoxicity, elevated levels of interleukin-8 (IL-8) proteins and antioxidant gene expression in bronchial epithelial (BEAS-2B) cells [25]. However, although these studies provide valuable insights into the respiratory toxicity of MNPs, most of the reported studies do not capture the full complexity of MNPs exposure, required for proper risk assessment.

First of all, in the absence of environmentally relevant reference material, most available research is focused on commercial spherical PS particles [26]. These homogeneous particles are produced via suspension polymerization of styrene, stabilized with surfactants and differ significantly from the MNPs present in the environment. Another major limitation is the restriction to cell lines in current studies. These conventional models, which are often cultured and exposed under submerged conditions, do not accurately recapitulate key characteristics of the bronchial epithelial barrier.

Therefore, in this study, we combined environmentally relevant MNPs with air-liquid interface (ALI) cultures of differentiated primary bronchial epithelial cells (PBEC). These fully differentiated PBEC cultures are comprised of various cell types, show active ciliary beating and mucus production, and therefore reliably mimic the morphological and functional characteristics of the bronchial epithelium *in vitro* [27]. We hypothesized that PBEC cultures derived from individuals with pre-existing pulmonary diseases (COPD) are more sensitive to MNPs exposure compared to PBEC cultures derived from individuals without history of chronic lung diseases. To investigate this, ALI cultures of PBEC of both non-COPD and COPD patients were exposed to MNPs of PVC, PP or PA-6.6. The MNPs implemented in this study were all produced via a standardized milling procedure by the MOMENTUM research consortium on Microplastics and Human Health, predominantly presenting a size range below  $1 \mu\text{m}$  (75–98%) [28].

Readouts in this study were all linked to key characteristics involved in COPD (as described above), and

included those related to inflammation, antioxidant response, apoptosis, autophagy, barrier disruption and airway remodeling. Understanding the impact of MNPs on bronchial epithelial cells may help identifying potential respiratory health risks of MNPs in health and disease.

## Materials and methods

### Applied particles and preparation of working suspensions

Copper (II) oxide (CuO) nanoparticles < 50 nm (Sigma-Aldrich, St. Louis, USA) were dispersed in MilliQ-water (MQ) via probe-sonication, as previously described [29]. MNPs of PVC(CAS: 9002-86-2), PP/Talc (CAS: 26063-22-9), PA-6.6 (CAS:63428-84-2) and talc particles (CAS:14807-96-6) were produced by cryo-milling, separated by size, and supplied in suspension in 1-propanol by the MOMENTUM consortium [28, 30]. The MOMENTUM MNPs in this study displayed a heterogeneous size distribution, although the majority of the particles was below 1  $\mu$ m. To specify, the fraction of nanoplastics was 98%, 89% and 75% for PVC, PP/Talc and PA respectively [30]. In the rest of this manuscript, we refer to these particles as MNPs. To improve the stability of the dispersions, predilutions of all particles were first prepared in 0.5% bovine serum albumin (BSA, Sigma-Aldrich)/Dulbecco's Phosphate Buffered Saline (dPBS, Thermo Fisher Scientific (Waltham, USA)) to increase steric repulsion. Thereafter, predilutions were further diluted to exposure concentrations with a final concentration of 0.05% BSA/dPBS and 1% 1-propanol in all exposure conditions.

### Characterization of MNPs

Stock suspensions of the amorphous MNPs used in this study have been extensively characterized before [30]. In the current study, static light scattering was conducted on the LA-960 particle size analyzer (HORIBA, Kyoto, Japan) after diluting the stock suspensions to 0.1 mg/mL in 0.05% BSA /1% 1-propanol/dPBS. Five measurements were performed under constant (minimal) movement at 23 °C, ~ 50% relative humidity. Refractive indices were set to 1.55–0.001 for PVC, and 1.50–0.001 for PA and 1.60–0.001 for PP/Talc respectively. The average median diameter was calculated using the LA-960 software (HORIBA) and presented as both number based ( $D_N$ ) as well as volume based ( $D_V$ ). Lastly, to exclude endotoxin contamination, we have determined endotoxin levels in PA, PVC, PP/Talc and talc suspensions (0.1 mg/mL in endotoxin free water) with the Pierce™ Chromogenic Endotoxin Quant Kit (Thermofisher scientific). This Limulus Amebocyte Lysate (LAL) assay enables to detect endotoxin levels between 0.01 and 1 EU/mL range.

### Culture of primary bronchial epithelial cells

PBEC were isolated from tissues collected by the Maastricht Pathology Tissue Collection (MPTC). All patients gave their informed consent. In addition, approval for using the tissue for research purposes was provided by both the scientific board of the MPTC (MPTC2010-019) and the local Medical Ethics Committee (METC 2017-0087). Furthermore, tissues were stored and handled following the 'Human Tissue and Medical Research: Code of conduct for responsible use' (2011) ([www.coreon.org](http://www.coreon.org)), and the guidelines of ethical framework of patient care at Maastricht University Medical Center+ (MUMC+). Isolation, culture and characterization of cells was conducted by the Primary Lung Culture (PLUC) facility at the MUMC + as previously described [31, 32]. Cells were acquired from resected lung tissue of three GOLDII COPD patients, as well as from three non-COPD patients without known history of chronic lung diseases who underwent surgery for solitary pulmonary nodules. All donors were diagnosed with non-small cell lung cancer (NSCLC) adenocarcinoma, other patient characteristics are described in Supplementary Table S1.

PBEC of passage 1 were thawed, seeded, expanded and seeded in 12-well cell culture transwell inserts with a polyethylene terephthalate membrane, pore size 0.4  $\mu$ m (CellQART, Northeim, Germany) as previously described [32]. After 4–7 days of submerged culture, cells were air-lifted and maintained at ALI for 29–31 days at 37 °C and 5% CO<sub>2</sub> until exposure experiments. The transepithelial electrical resistance (TEER) was monitored during differentiation using an epithelial tissue voltohmometer (World Precision Instruments, Sarasota, USA). TEER values were corrected for background (cell-free insert) and surface area. Furthermore, differentiation of PBEC was validated by characterizing epithelial cell type-specific markers using Real-time polymerase chain reaction (qPCR) and immunohistochemistry staining [29, 32]. Supplementary tables S2 and S3 present primers and antibodies applied in this study.

### Exposure of PBEC to MNPs and nanoparticles

Airlifted PBEC cultures of both non-COPD as well as COPD patients were exposed to particle suspensions (see paragraph 2.1) at the apical side via a single 20  $\mu$ L droplet. Applied doses were expressed in  $\mu$ g/cm<sup>2</sup>, based on the cell surface area of the insert (1.1 cm<sup>2</sup>). Applied doses for MNPs were 0.6  $\mu$ g/cm<sup>2</sup>, 3  $\mu$ g/cm<sup>2</sup>, or 15  $\mu$ g/cm<sup>2</sup>. PP/Talc MNPs contained approximately 30 wt% talc, therefore tested talc concentrations were 0.18  $\mu$ g/cm<sup>2</sup>, 0.9  $\mu$ g/cm<sup>2</sup>, or 4.5  $\mu$ g/cm<sup>2</sup>, corresponding with 30% of the PP/Talc dose [30]. For CuO, the applied dose was 1.39  $\mu$ g/cm<sup>2</sup>, corresponding with the dose inducing IL-8 secretion in previous studies [29]. For COPD-patient derived PBEC exposures, we included a single dose, corresponding with

the highest dose tested for non-COPD PBEC. An unexposed incubator-control was included in all experiments. Cells were placed back in the incubator directly after exposure. Following 24 h incubation, an apical wash with dPBS was collected, as well as basolateral medium and cell lysate in TRIzol™ reagent (Invitrogen).

#### Analyzing distribution of MNPs

The environmentally relevant PVC, PP/Talc and PA MNPs implemented in this study were non-labelled. Fluorescent PS MNPs allowed us to characterize distribution of MNPs in PBEC and confirm active cilia beating of the cultures. First, differentiated non-COPD PBEC were exposed to 4.5 ng/cm<sup>2</sup> unmodified red fluorescent PS particles (size 2.1 µm) (Magsphere, Pasadena, USA) via a single 10 µL droplet. Subsequently, 5–10 min after exposure, distribution of the PS particles was analyzed by studying motion of the fluorescent beads up to 2.5 h after exposure, as described previously [32].

#### Cytotoxicity assay

Lactate dehydrogenase (LDH) analysis was conducted on the apical wash, to determine cytotoxicity according to manufacturer's specifications (Cytotoxicity Detection Kit (LDH) Roche AG). Cytotoxicity was expressed as percentage of LDH max, which was derived by incubating cells for 10 min in Triton-X-100/PBS (2%).

#### Inflammatory protein secretion

IL-8 protein levels were quantified separately in both the apical wash as well as the basolateral medium, using the Human IL-8/CXCL8 ELISA DuoSet kit according to manufacturer's specifications (R&D Systems, Minneapolis, USA). A SpectraMax iD3 Multi-Mode Microplate reader (Molecular Devices) was used for absorbance measurements. IL-8 protein levels were corrected for different apical/basolateral volumes, subsequently combined and expressed as total IL-8 protein secreted per insert.

#### RNA isolation and real-time quantitative PCR

Total RNA from PBEC was extracted by lysis in TRIzol™ reagent (Invitrogen) and further processed into cDNA, as previously described [29]. qPCR was performed on the CFX Opus 384 Real-Time PCR System (Bio-Rad, Hercules, USA) [25]. Primers are listed in Supplementary Table S2. Gene expression was quantified with the CFX Maestro software v2.3 (Bio-Rad) and LinRegPCR software 2014 and normalized using the geometric mean of four housekeepers: (beta-actin (*ACTB*), beta-2 microglobulin (*B2M*), Cyclophilin A (*CYPA*), and ribosomal protein L13A (*RPL13A*) [33]. Gene expression data was expressed as normalized gene expression level (Arbitrary unit), or

as fold change between normalized gene expression levels between the exposed cultures and vehicle control.

#### Transmission electron microscopy

We deployed transmission electron microscopy (TEM) in an attempt to study PA MNPs uptake, and to assess potential ultrastructural changes after PA exposure. Differentiated PBEC derived from non-COPD (two donors) and COPD (two donors) subjects were exposed to 3 µg/cm<sup>2</sup> PA MNPs as described above (paragraph '2.4. Exposure of PBEC to MNPs and nanoparticles'). 24 h after exposure, samples were incubated with fixative (1.5% glutaraldehyde/0.067 M cacodylate/1% sucrose, pH 7.4) for 2 min at room temperature. After incubation, the fixative was refreshed with new fixative. 24 h post fixation, inserts were washed with washing buffer (0.1 M cacodylate, pH 7.4) and incubated for 1 h with osmium tetroxide in the same buffer containing 1.5% potassium ferricyanide in the dark at 4 °C. Specimens were washed several times with washing buffer, till the solution was clear. Dehydration was performed in a series of ethanol solutions of increasing concentration. Subsequently, samples were infiltrated with Epon resin, embedded in the same resin and polymerized at 60 °C for 48 h. Ultrathin sections of 70 nm were obtained using a Leica Ultracut UCT ultramicrotome (Leica Microsystems, Vienna) and mounted on Formvar-coated copper grids. They were stained with 2% uranyl acetate in ethanol and lead citrate. TEM was conducted at the University of Hasselt (Belgium) using a JEOL JEM-1400Flash microscope (JEOL Ltd., Akishima, Tokyo, Japan) operated at 80 kV. High-resolution images (5120 × 3840 pixels) were acquired with an EMSIS Xarosa camera (EMSIS GmbH, Münster, Germany) controlled by RADIUS 2.1 software (Build 20150). For the four donors, we first created overview pictures at lower magnification, to explore morphological alterations present, and general membrane integrity. Thereafter, more detailed images were acquired (up to 10.000x magnification).

#### Statistical analysis

All data are obtained from three independent exposure experiments, all performed in technical triplicate. GraphPad Prism version 10.2.3 was used to perform statistical analyses. Normality and homogeneity of variance of the data was checked using a Shapiro-Wilk test and Brown-Forsythe test respectively. To study differentiation and compare base-level expressions in unexposed COPD-PBEC vs. unexposed non-COPD PBEC, an ANOVA with Bonferroni's multiple comparisons test was performed. For exposures performed in dose-response (non-COPD PBEC), statistical differences between particle-exposed cultures versus vehicle-exposed cultures were tested using an ordinary one-way ANOVA with Dunnett's multiple comparisons test (normally distributed data)

or a Kruskal-Wallis test (non-normally distributed data). For PBEC derived from COPD patients, and CuO exposed cultures (not tested in dose-response) statistical differences compared to the vehicle are tested using a two-tailed unpaired t-test with Welch's correction or Mann-Whitney test. Data are presented as mean values for each donor or biological replicate  $\pm$  SD. p-values  $< 0.05$  were considered as significant and indicated as \* ( $P < 0.05$ ), \*\* ( $P < 0.01$ ), \*\*\* ( $P < 0.001$ ) or \*\*\*\* ( $P < 0.0001$ ).

## Results

### Particle characteristics

Physical and chemical characterization of the MNPs used in this study (previously published) revealed that all particles displayed an amorphous morphology (scanning electron microscopy), and a negative surface charge (zeta potential) in 1-propanol [29, 30]. In addition, the presence of impurities, including metals from the milling process, was determined to be  $< 1$  wt% (X-ray Fluorescence or Inductively coupled plasma mass spectrometry) [30]. The endotoxin content for the MNPs was considered negligible, since all values were below the detection limit of the LAL assay ( $< 0.01$  EU/mL in 0.1 mg/mL particle suspension). The size distribution of MNPs in 1-propanol was close to the primary particle size (Table 1 [30]). As it is well-established that experimental conditions, like use of cell culture medium and sample preparation, can influence particle characteristics and behavior, we also characterized the size distribution of the MNPs in the (droplet) exposure medium. As displayed in Table 1, all MNPs displayed a broader size distribution as well as an increase in median size after dispersion in PBS/0.05%BSA/1% 1-propanol, indicating particle agglomeration and/or protein-surface interactions (Table 1, Figure S1).

### Characterization of PBEC from non-COPD and COPD Patients

PBEC were isolated from three COPD patients (GOLD stage II) and three non-COPD patients. Presence or absence of COPD was based on spirometric assessment

**Table 1** Median diameter of particles. The median diameter ( $D_N$  number basis and  $D_V$  volume basis) was measured for Polypropylene/Talc (PP/Talc), Polyvinylchloride (PVC) and Polyamide-6.6 (PA) in 1-propanol and PBS/0.05%BSA/1% 1-propanol, using static light scattering. \* Size distributions in 1-propanol are derived from earlier publications [28, 30]

	1-propanol*		PBS/ 0.05%BSA/ 1% 1-propanol	
	$D_N$ ( $\mu\text{m}$ )	$D_V$ ( $\mu\text{m}$ )	$D_N$ ( $\mu\text{m}$ )	$D_V$ ( $\mu\text{m}$ )
PP/Talc	0.40	5.83	5.87	9.92
PVC	0.21	5.72	6.31	11.0
PA	0.68	5.60	2.28	3.90

of the Tiffeneau index (COPD: FEV<sub>1</sub>: forced expiratory volume in the first second/ FVC: forced vital capacity  $< 70\%$  of predicted). Patient characteristics are displayed in Table S1. In summary, all subjects were ex-smokers with an age range of 57–73. All donors were male except for non-COPD donor 1.

Regarding the characterization of the PBEC cultures of these subjects, we observed that TEER values of PBEC of all donors increased during differentiation (Fig. 1A-B). However, some donor variability was observed, with TEER levels stabilizing at a lower level for all COPD donors compared to non-COPD donors after completion of the differentiation period. In addition, non-COPD donor 3 failed to reach the TEER levels that were observed in the other two non-COPD donors. Since barrier function is highly dependent on tight junctions, we investigated potential differences in the mRNA expression of epithelial junction proteins in non-COPD patients and COPD patients. Both PBEC from COPD and non-COPD established tight junctions as observed by TEM (Fig. 1G). Compared to non-COPD donors, in general we observed a lower expression of tight junction proteins in PBEC from COPD patients, with CLAUDIN 4 (*CLDN4*) expression in COPD subjects being significantly lower compared to non-COPD subjects (FC = 0.36,  $p = 0.02$ ) (Fig. 1C-F).

For all cultures, we observed a significant increase in mRNA transcript levels of a ciliated cell marker (Forkhead box J1; *FOXJ1*), goblet cell marker (Mucin-5AC; *MUC5AC*) and club cell secretory marker (Secretoglobin Family 1 A Member 1; *SCGB1A1*) in differentiated cultures compared to undifferentiated cultures. In contrast, mRNA transcript levels of basal epithelial cell markers (Keratin 5; *KRT5* and tumor protein P63; *TP63*) decreased substantially during differentiation in all cultures (Figure S2A-D). With regard to the comparison of COPD cultures vs. non-COPD cultures, for most cell-type-specific markers we observed no significant baseline differences in mRNA expression in undifferentiated COPD vs. non-COPD cultures. Baseline differences between COPD and non-COPD PBEC are summarized in Supplementary Table S4. Interestingly, *KRT5* mRNA levels were significantly lower when comparing undifferentiated cultures of COPD patients vs. non-COPD patients (FC = 0.43,  $p = 0.05$ ) (Figure S2A). In differentiated cultures, no significant differences in gene expression of epithelial cell markers were observed in COPD vs. non-COPD cultures (Figure S2). All cultures visually produced mucus, although we observed donor variability in the amount of mucus produced. Immunohistochemistry confirmed the presence of club cells, ciliated cells and mucus-producing cells after completion of the differentiation program in all cultures (Figure S3). Although not quantified, Scgb1a1 protein levels (as a marker for club

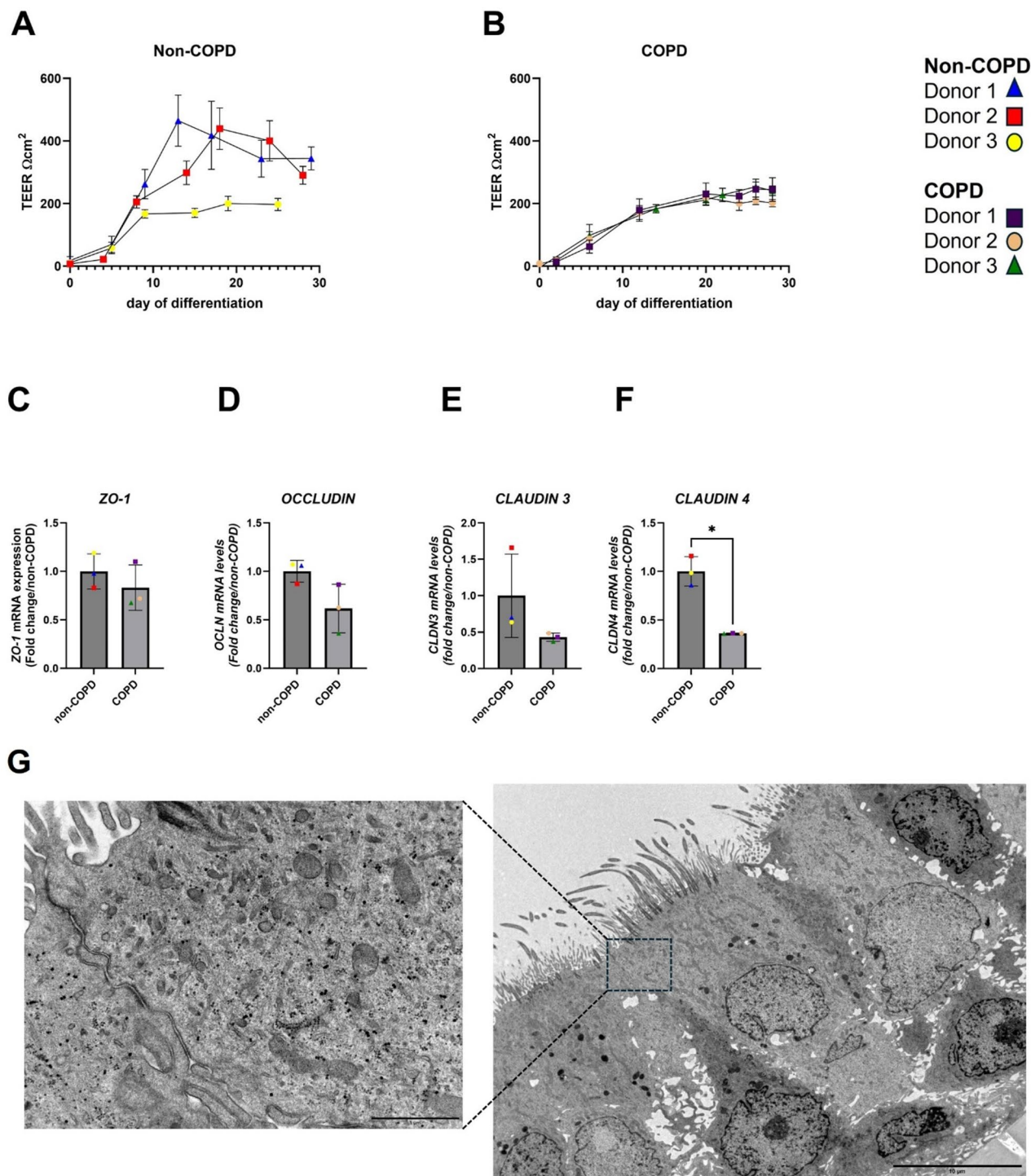


**Fig. 1** Barrier integrity of primary bronchial epithelial cells (PBEC). Transepithelial electrical resistance (TEER) was determined during differentiation of non-COPD (A) and COPD (B) PBEC. mRNA expression of markers for tight junction proteins in unexposed differentiated cultures of non-COPD and COPD PBEC, expressed as fold change compared to non-COPD. Zonula occludens (ZO)-1 (C), Occludin (OCLN) (D), Claudin 3 (CLDN3) (E) and Claudin 4 (CLDN4) (F). Each data point represents the mean of a technical triplicate of an individual donor.  $*P < 0.05$  compared to non-COPD PBEC. Transmission electron microscopy (TEM) image of PBEC, with tight junctions localized intercellularly on the apical side (G)

cells) appeared to be lower for COPD donors 1 and 2, compared to the other (non-COPD) donors.

Collectively, this data indicated that all PBEC cultures from both non-COPD and COPD donors formed an intact, confluent, pseudostratified multi-cellular epithelial barrier upon differentiation. Although we observed some donor variability in morphology and cellular composition, no striking differences were observed when comparing COPD and non-COPD cultures.

### Particle distribution

Prior to toxicity experiments, we visualized deposition and distribution dynamics of MNPs in PBEC using fluorescent PS beads. With regard to deposition characteristics of suspensions of MNPs in a droplet on ALI cultures of PBEC, we observed that these PS beads were swirled around across the surface of these cultures due to ciliary beating (Supplemental movies). In addition, we observed that PS particles were trapped in the mucus droplet that is continuously produced by the goblet cells.

### MNPs do not impact cell viability in primary bronchial epithelial cells

24 h after exposure, cytotoxicity was assessed based on LDH release by PBEC cultures. For both non-COPD as well as COPD PBEC, cell viability was not significantly altered after exposure to MNPs or talc for any of the doses tested. In contrast to non-COPD PBEC, cell viability in COPD PBEC was significantly decreased ( $p=0.0309$ ) after CuO exposure (Fig. 2).

Since the LDH assay is particularly useful for detecting necrosis and late-stage apoptosis, we also investigated the effects of MNPs on transcription of BCL2 Associated X (*BAX*), a regulator of the early-stages of apoptosis. In general, no significant change was observed in *BAX* expression after exposure to nanoparticles or MNPs, although individual changes were observed (Fig. 2C, D). More specifically, in all non-COPD donors PVC and PA increased *BAX* expression, with the highest response observed for non-COPD donor 2 (Fig. 2C). In contrast, PP/Talc strongly decreased *BAX* expression in this non-COPD donor. PP/Talc also reduced *BAX* expression in two COPD-donors (Fig. 2D).

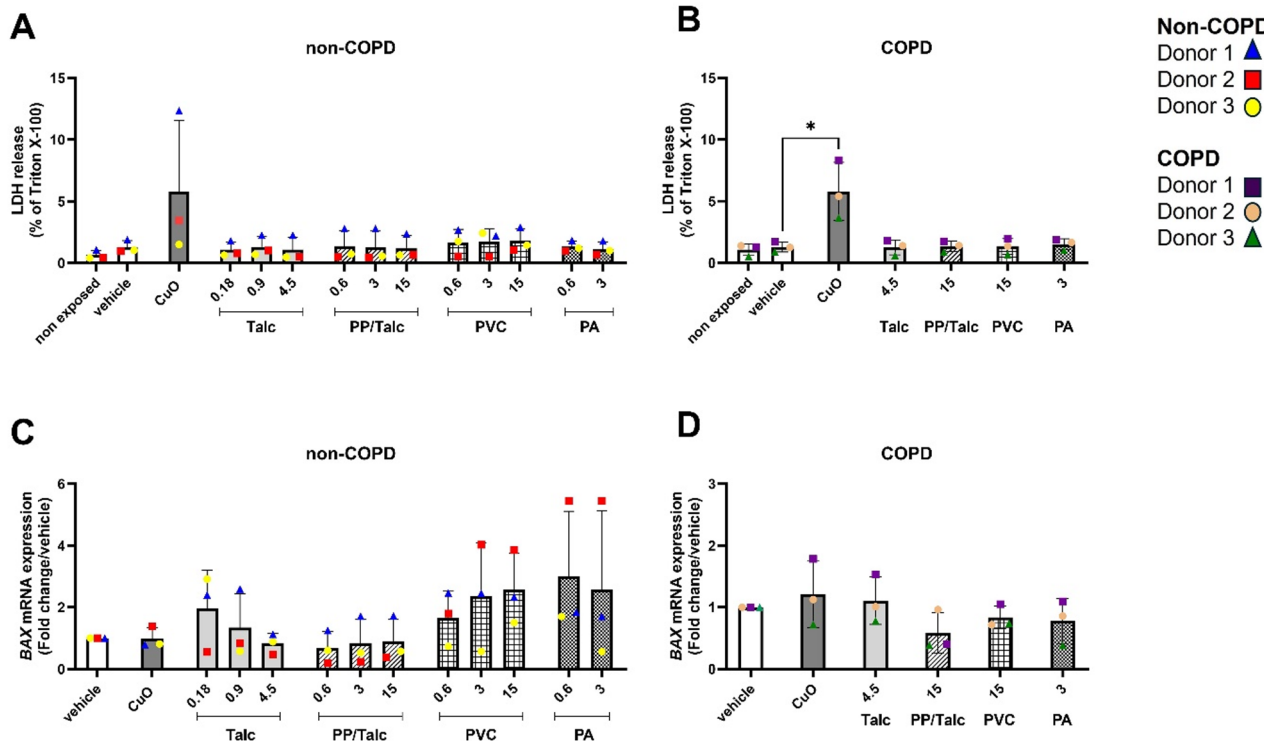


**Fig. 2** Effect of MNPs, CuO and talc on cell death. Differentiated cultures of primary bronchial epithelial cells non-COPD (A) patients ( $n=3$ ) and COPD (B) patients ( $n=3$ ) were exposed to the vehicle control (dPBS, 0.05% BSA, 1% 1-propanol), 1.39  $\mu\text{g}/\text{cm}^2$  copper(II) oxide (CuO), talc, polypropylene/talc (PP/Talc), polyvinylchloride (PVC) or polyamide-6.6 (PA) particles in dPBS, 0.05% BSA, 1% 1-propanol. Nominal doses are displayed on the X-axis, in  $\mu\text{g}/\text{cm}^2$ . Release of lactate dehydrogenase (LDH) was measured after 24 h at the apical side and presented as mean percentage of maximum LDH release (cells treated with 2% Triton X-100)  $\pm$  SD (A, B). BCL2 Associated X (*BAX*), Apoptosis Regulator, mRNA levels of the same cultures are shown as fold change compared to the vehicle control (C, D). For all experimental conditions, each data point represents the mean of a technical triplicate of an individual donor. \* $P<0.05$  compared to vehicle control

Additionally, we investigated the effects of MNPs on the expression of key molecules involved in autophagy, since this cellular survival mechanism and quality control process is highly connected to cell death mechanisms [34]. Overall, mRNA levels of both GABA type A receptor-associated protein like 1 (*GABARAPL1*) and sequestosome-1 (*SQSTM1/p62*) were not significantly affected in PBEC, although again we observed high variabilities between donors (Figure S4). In non-COPD donor 1, MNP exposure reduced expression of *SQSTM1*, in all applied doses (Figure S4A, C). In contrast, both autophagy regulators were strongly upregulated in PBEC cultures from donor 3, exposed to PA and PVC MNPs. In non-COPD donor 2 *SQSTM1* was downregulated by 15  $\mu\text{g}/\text{cm}^2$  PP/Talc, while low doses (0.6  $\mu\text{g}/\text{cm}^2$ ) of both PVC and PA MNPs increased autophagy marker *GABARAPL1*.

Regarding COPD-PBEC, PP/Talc decreased one or both autophagy markers in two donors. In COPD-donor 3, *GABARAPL1* mRNA levels were also decreased after PA exposure. The autophagy markers were not affected in COPD donor 2 (Figure S4B, D). To summarize, while MNPs displayed no profound cytotoxicity in PBEC, key

regulators of cellular apoptosis and survival were affected in a donor-dependent way.

#### MNPs do not impact transcription and secretion of IL-8

In addition to assessing potential MNPs-induced cytotoxicity, IL-8 protein secretion as well as gene expression were measured after exposure of PBEC cultures to MNPs or CuO. IL-8 is a pro-inflammatory factor that has been recognized to play a significant role in acute lung injury and the development and exacerbations of COPD [35]. In general, we did not observe significant differences in baseline levels of IL-8 secretion in cultures from COPD-patients vs. non-COPD patients (Fig. 3A-B). Furthermore, droplet exposure of PBEC cultures at the apical surface did not result in significant changes in IL-8 secretion. CuO, included as positive control, induced significant levels of IL-8 secretion (Fig. 3A-B) and increased C-X-C motif chemokine ligand 8 (*CXCL8*) mRNA expression (Fig. 3C-D) in all donors. It has to be mentioned however that, although at the group level MNP exposure did not result in any significant changes in IL-8 secretion or *CXCL8* expression, some biological variation with regard to responsiveness of individual donors

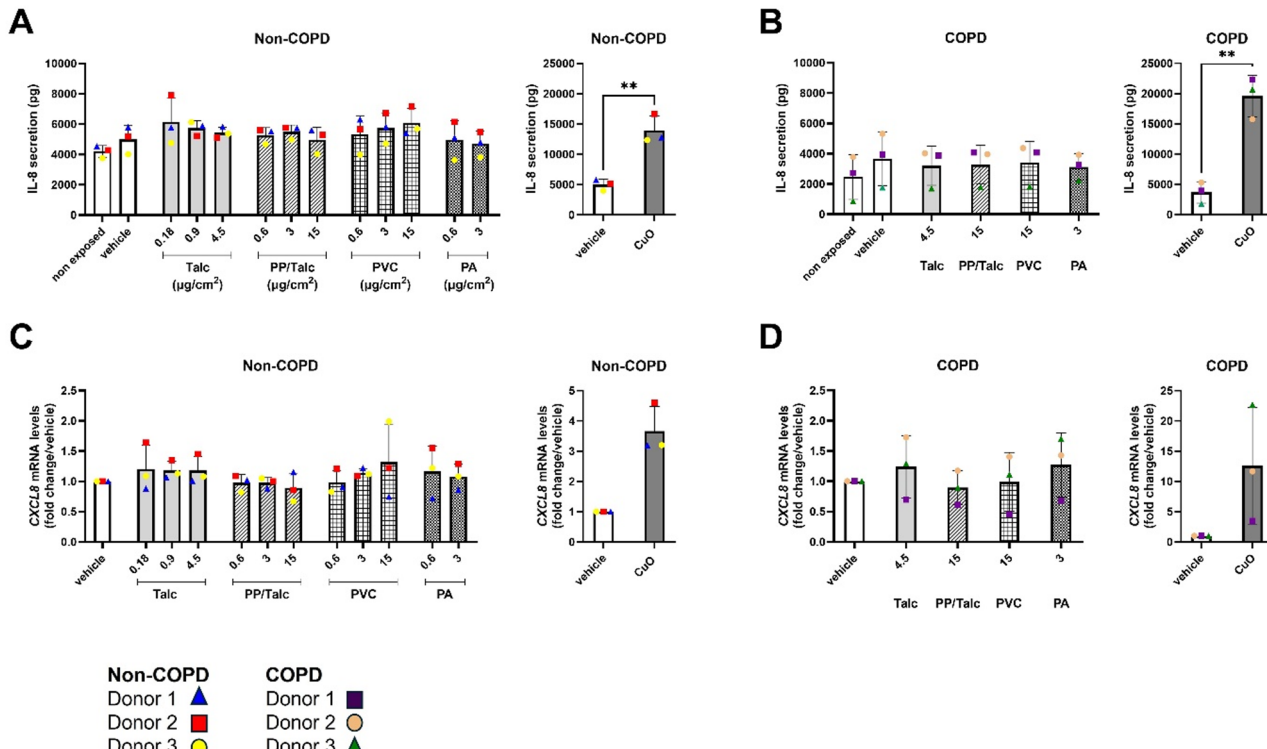


**Fig. 3** Effect of MNPs and nanoparticles on transcription and secretion of IL-8. Differentiated cultures of primary bronchial epithelial cells non-COPD patients ( $n=3$ ) and COPD patients ( $n=3$ ) were exposed to the vehicle control (dPBS, 0.05% BSA, 1% 1-propanol), 1.39  $\mu\text{g}/\text{cm}^2$  copper (II) oxide (CuO), talc, polypropylene/talc (PP/Talc), polyvinylchloride (PVC) or polyamide-6,6 (PA) particles in dPBS, 0.05% BSA, 1% 1-propanol. Nominal doses are displayed on the X-axis, in  $\mu\text{g}/\text{cm}^2$ . For all experimental conditions, each data point represents the mean of a technical triplicate of an individual donor IL-8 protein levels (apical and basolateral) were assessed with ELISA and reported as total absolute IL-8 protein levels per insert (A, B). CXCL8 mRNA levels of the same cultures are shown as fold change compared to the vehicle control (C, D). \*\* $P<0.01$  compared to vehicle control

was observed. For example, non-COPD donor 3 showed a dose-dependent increase in *CXCL8* mRNA expression (up to FC: 2.0) after PVC MNP exposure (Fig. 3C).

#### MNPs modulate antioxidant gene expression

In addition to inflammation, oxidative stress is a major driving mechanism of COPD airway pathology and both processes have been described to be interconnected [36]. To explore this, we investigated the expression of two major antioxidant enzymes, both crucial in the cellular defense against oxidative stress. The expression of superoxide dismutase 1 (*SOD1*) did not change substantially after exposure to MNPs or nanoparticles, apart from non-COPD donor 2 (Fig. 4A, B). For this donor, *SOD1* mRNA levels were increased up to 8-fold by PVC MNP exposure and up to 9-fold by PA MNP exposure. Small changes were observed for non-COPD donor 3, where the lowest dose of PA MNPs increased *SOD1* mRNA levels. (Fig. 4A). Similar trends were observed for *SOD2* expression in non-COPD donors, where again donor 2 demonstrated a strong increase in *SOD2* expression after PVC and PA MNP exposure. In contrast, PP/Talc reduced *SOD2* levels in this donor.

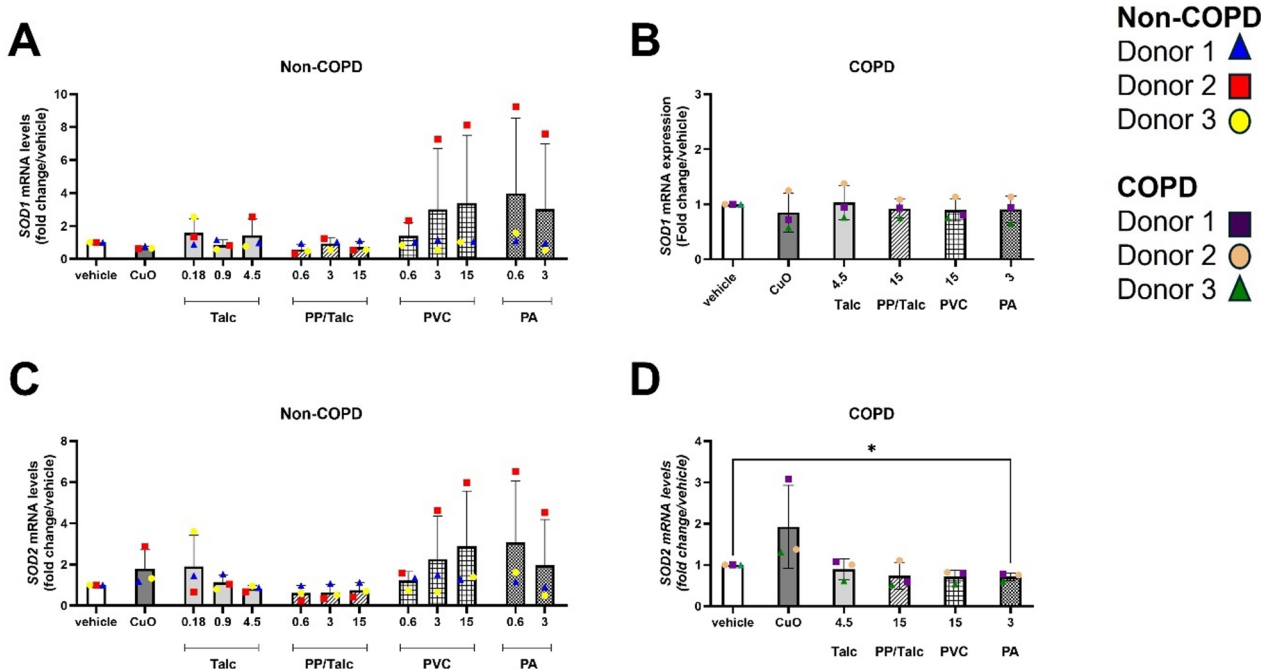
In non-COPD donor 3, a low PA dose (0.6  $\mu\text{g}/\text{cm}^2$ ) increased *SOD2* expression, while 3  $\mu\text{g}/\text{cm}^2$  PA reduced

*SOD2* levels in this donor. In non-COPD donor 1, only 3  $\mu\text{g}/\text{cm}^2$  PVC increased *SOD2* mRNA levels.

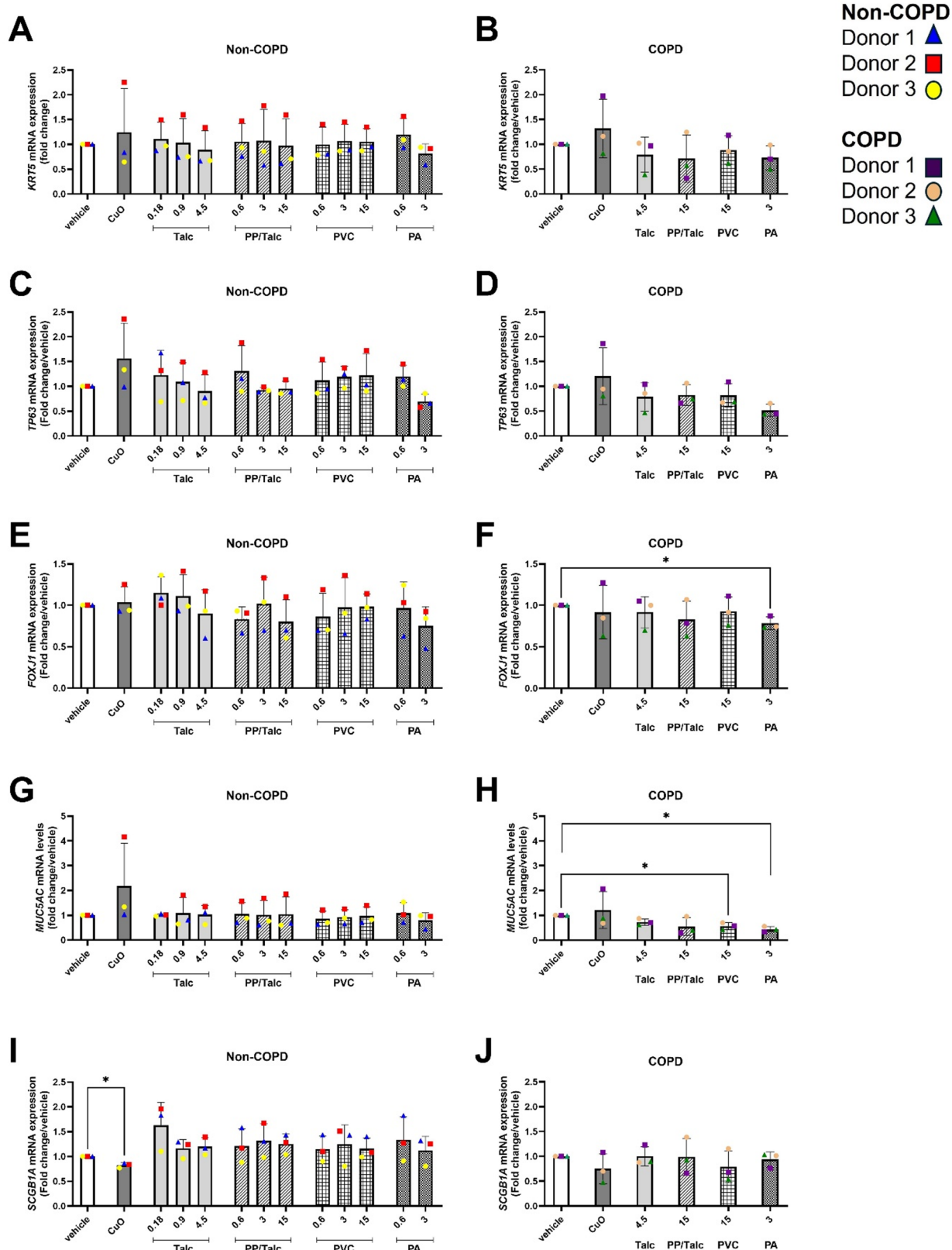
In COPD PBEC, *SOD2* was significantly downregulated in all donors after exposure to 3  $\mu\text{g}/\text{cm}^2$  PA (FC = 0.72,  $p = 0.03$ ) (Fig. 4C, D). These results suggest that, although with significant inter-donor variability, MNPs can activate an antioxidant response in non-COPD PBEC, this response might be impaired in COPD PBEC.

#### MNPs alter the expression of epithelial cell markers in COPD PBEC

Next, we investigated if MNP exposure affected gene expression levels of several epithelial cell markers associated with specific cells present in the differentiated multicellular bronchial epithelial cell layer (basal-, ciliated, goblet- and club cells). In non-COPD cultures, taking all donors together, there was no significant change in gene expression levels of any of the cell type-specific markers in response to any of the MNPs tested. However, we did observe some donor-specific responses to MNPs (Fig. 5). More specifically, in donor 2, in contrast to the other two non-COPD donors, we observed increased expression of basal cell markers (*KRT5* and/or *TP63*) after exposure to PVC, PP/Talc, talc and CuO (Fig. 5A, C). Remarkably, in the same donor as well as for donor 1, gene expression of basal cell markers decreased after PA MNP exposure



**Fig. 4** Effect of MNPs and nanoparticles on transcription of antioxidant enzymes. Differentiated cultures of primary bronchial epithelial cells non-COPD patients ( $n=3$ ) and COPD patients ( $n=3$ ) were exposed to the vehicle control (dPBS, 0.05% BSA, 1% 1-propanol), 1.39  $\mu\text{g}/\text{cm}^2$  copper (II) oxide (CuO), talc, polypropylene/talc (PP/Talc), polyvinylchloride (PVC) or polyamide-6,6 (PA) particles in dPBS, 0.05% BSA, 1% 1-propanol. Nominal doses are displayed on the X-axis, in  $\mu\text{g}/\text{cm}^2$ . For all experimental conditions, each data point represents the mean of a technical triplicate of an individual donor. superoxide dismutase 1 (*SOD1*) (A, B) and superoxide dismutase 2 (*SOD2*) (C, D) mRNA levels as fold change compared to the vehicle control.  $*p < 0.05$  compared to vehicle control

**Fig. 5** (See legend on next page.)

(See figure on previous page.)

**Fig. 5** Effect of MNPs and nanoparticles on epithelial cell markers. Differentiated cultures of primary bronchial epithelial cells non-COPD patients ( $n=3$ ) and COPD patients ( $n=3$ ) were exposed to the vehicle control (dPBS, 0.05% BSA, 1% 1-propanol), 1.39  $\mu\text{g}/\text{cm}^2$  copper(II) oxide (CuO), talc, polypropylene/talc (PP/Talc), polyvinylchloride (PVC) or polyamide-6,6 (PA) particles in dPBS, 0.05% BSA, 1% 1-propanol. Nominal doses are displayed on the X-axis, in  $\mu\text{g}/\text{cm}^2$ . mRNA expression of epithelial cell type-specific markers in exposed cultures. Basal cell markers: Keratin 5 (*KRT5*) (**A, B**), tumor protein p63 (*TP63*) (**C, D**). Ciliogenesis marker: Forkhead box J1 (*FOXJ1*) (**E, F**). Goblet cell marker: Mucin-5AC (*MUC5AC*) (**G, H**). Club cell secretory marker: Secretoglobin Family 1 A Member 1 (*SCGB1A1*) (**I, J**). For all experimental conditions, each data point represents the mean of a technical triplicate of an individual donor. \* $P<0.05$  compared to vehicle control

(Fig. 5A, C). This trend was also observed in PBEC from the COPD donors, where PA decreased *TP63* expression in all donors ( $FC=0.52$ ), although not statistically significant. The same dose of PA also decreased expression of ciliated cell marker, *FOXJ1* and *MUC5AC* in COPD-PBEC ( $FC=0.78$ ,  $p=0.04$  and  $FC=0.44$ ,  $p=0.01$ ). *MUC5AC* expression was also decreased in COPD-PBEC exposed to PVC MNPs, compared to the vehicle control ( $FC=0.57$ ,  $p=0.03$ ). For non-COPD PBEC, *FOXJ1* was downregulated in non-COPD donor 1, but not in the other two donors (Fig. 5E). In contradiction to CuO ( $FC=0.82$ ,  $p=0.03$  in non-COPD donors), no changes were observed in club cell marker *SCGB1A1* after MNP exposure (Fig. 5I, J).

In summary, exposure to MNPs, especially PA, impaired the expression of epithelial cell markers in COPD-derived PBEC. PA decreased the expression of cilia marker *FOXJ1*, as well as goblet cell marker *MUC5AC*. The most universal trend however, was observed on basal cell marker *TP63*, since this marker was downregulated by PA in all donors. For non-COPD donors, a variability in response between individual donors was observed.

#### MNPs impact gene expression of tight junction proteins

The primary function of the airway epithelium is to function as physical barrier for inhaled substances. TEM pictures of bronchial epithelial cells exposed to PA MNPs indicated cell-cell contacts were preserved after exposure, and no drastic cell detachment was observed (data not shown). However, on mRNA level, we did observe changes in genes encoding for proteins that are important in stabilizing tight junctions and maintaining proper barrier function. In more detail, PVC exposure increased Occludin (*OCLN*) expression in non-COPD PBEC, in a dose-dependent manner (Fig. 6C, FC up to 1.98,  $p=0.05$ ). In addition, PVC induced Claudin 3 (*CLDN3*) and *CLDN4* expression in non-COPD donor 3, whereas expression of these genes was decreased in the other two non-COPD donors (Fig. 6E, G). In general, PP/Talc decreased expression of genes coding for tight junction proteins in non-COPD PBEC, with only *CLDN3* being significantly different from the vehicle control (Fig. 6E,  $FC=0.45$ ,  $p=0.05$ ). For all COPD-PBEC cultures, PA (3  $\mu\text{g}/\text{cm}^2$ ) significantly decreased Zonula Occludens (*ZO*)-1 expression (Fig. 6B,  $FC=0.76$ ,  $p=0.01$ ), as well as *OCLN* (Fig. 6D,  $FC=0.75$ ,  $p=0.03$ ). In contrast, we did

not observe significant differences in gene expression of any of the tight junction proteins tested for non-COPD PBEC after PA exposure, although again we observed high donor variability (Fig. 6A, C, E, G).

#### PA MNPs induce morphological changes in PBEC

Given that PA, more than the MNPs from other polymers, modulated the expression of cell-type specific genes as well as genes involved in cell-cell interaction, TEM was applied to explore potential PA-induced morphological changes. Preliminary observations in PBEC of two non-COPD donors and two COPD-donors revealed clustered, electron-lucent vesicles in ciliated cells following exposure to PA MNPs in all four donors studied. These vesicles, located near to the nucleus and highlighted by red circles in Fig. 7 (Figure S5 for higher magnification, as well as other PA-exposed donors), were absent in vehicle control samples. To specify, these clustered vesicles were visible in exposed cultures of both COPD donors, as well as non-COPD donor 2. For non-COPD donor 3 clustered vesicles were also observed, but generally more distributed through the cell. The emergence of these intracellular vesicle clusters suggests potential alterations in endocytic or lysosomal pathways, or the activation of a cellular stress response, but this remains to be established.

#### Discussion

To our knowledge, this is the first study that compared the acute response of differentiated PBEC from COPD patients and non-COPD patients to MNPs of different polymers. We detected considerable variation in response to MNPs between donors, especially in non-COPD PBEC. Although, none of the MNPs we investigated elicited a profound cytotoxic or an inflammatory response, we did observe MNPs modulated antioxidant gene expression, as well as key regulators of cellular apoptosis and survival in a donor-dependent way. Furthermore, PA MNPs significantly modulated the expression of genes encoding for tight junction proteins and epithelial cell markers in COPD-PBEC. This suggests changes in the cellular composition and integrity of the bronchial epithelial barrier resulting PA MNP exposure.

This study aimed to collect hazard data for environmentally relevant MNPs. Extrapolating environmental MNP exposure to an in vitro dose, remains challenging. Due to analytical limitations, airborne nanoplastic

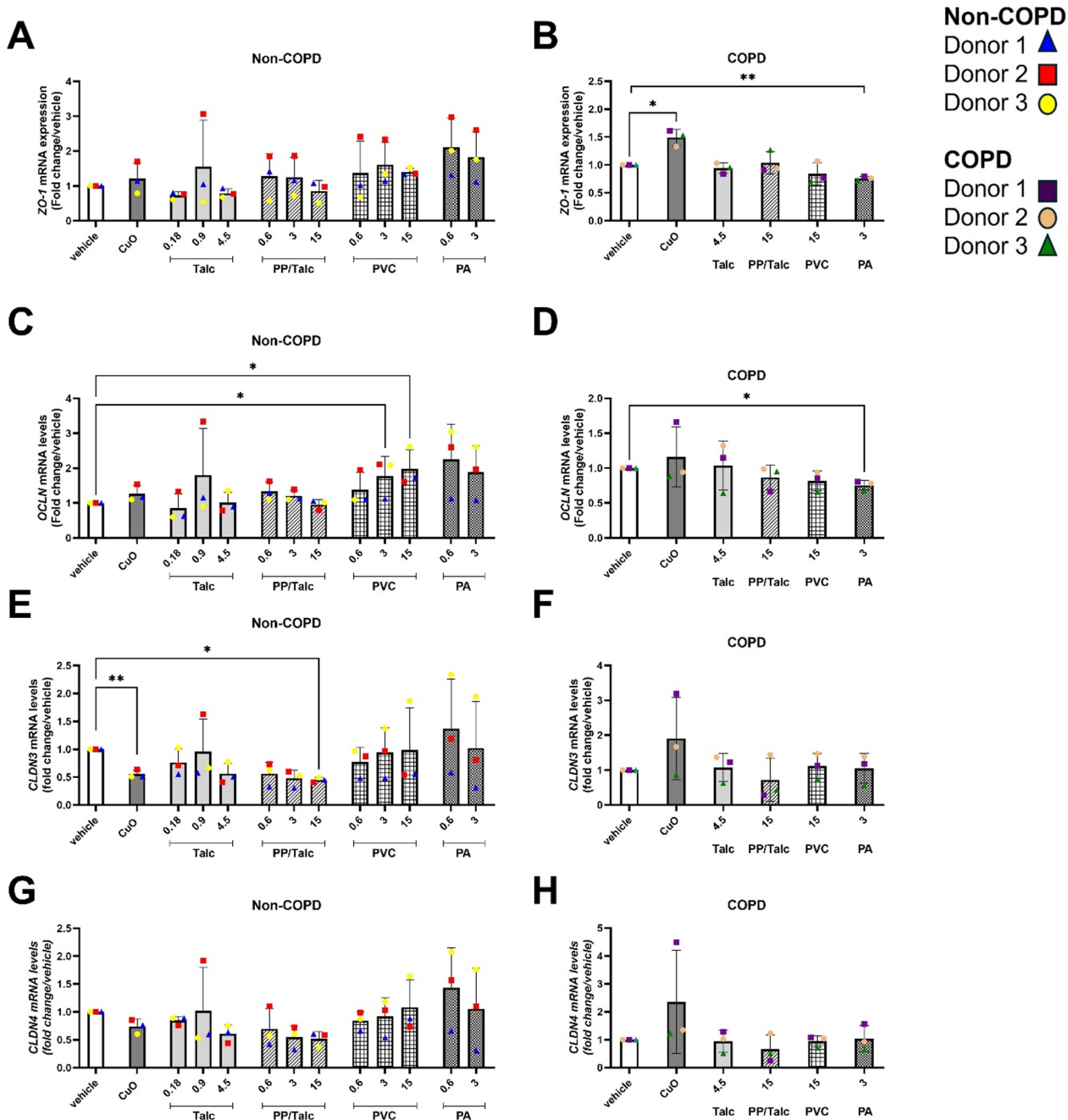


**Fig. 6** Effect of MNPs and nanoparticles on tight junction gene expression. Differentiated cultures of primary bronchial epithelial cells non-COPD patients ( $n=3$ ) and COPD patients ( $n=3$ ) were exposed to the vehicle control (dPBS, 0.05% BSA, 1% 1-propanol), 1.39  $\mu\text{g}/\text{cm}^2$  copper(II) oxide (CuO), talc, polypropylene/talc (PP/Talc), polyvinylchloride (PVC) or polyamide-6.6 (PA) particles in dPBS, 0.05% BSA, 1% 1-propanol. Nominal doses are displayed on the X-axis, in  $\mu\text{g}/\text{cm}^2$ . mRNA expression of tight junctional proteins in exposed cultures: zonula occludens (ZO-1) (A, B), Occludin (OCLN) (C, D), Claudin 3 (CLDN3) (E, F) and Claudin 4 (CLDN4) (G, H). For all experimental conditions, each data point represents the mean of a technical triplicate of an individual donor. \* $P<0.05$ , \*\* $P<0.01$  compared to vehicle control

exposure levels can currently only be extrapolated from data sets on larger sized particles. Furthermore, exposure levels are highly variable among individuals and can rise during occupational settings. Based on environmental samples, Eberhard et al., estimated the maximum occupational exposure to airborne microplastics ( $> 1 \mu\text{m}$ ) at

a plastic recycling facility to be 22,531 microplastics/kg body weight per day [3]. Assuming an equal distribution over the airways ( $2471 \pm 320 \text{ cm}^2$ ), this would correspond to  $710\text{--}922$  particles/ $\text{cm}^2$ , approximately two orders of magnitude lower than the lowest dose applied in this study [3, 37]. Since the purpose of this study was

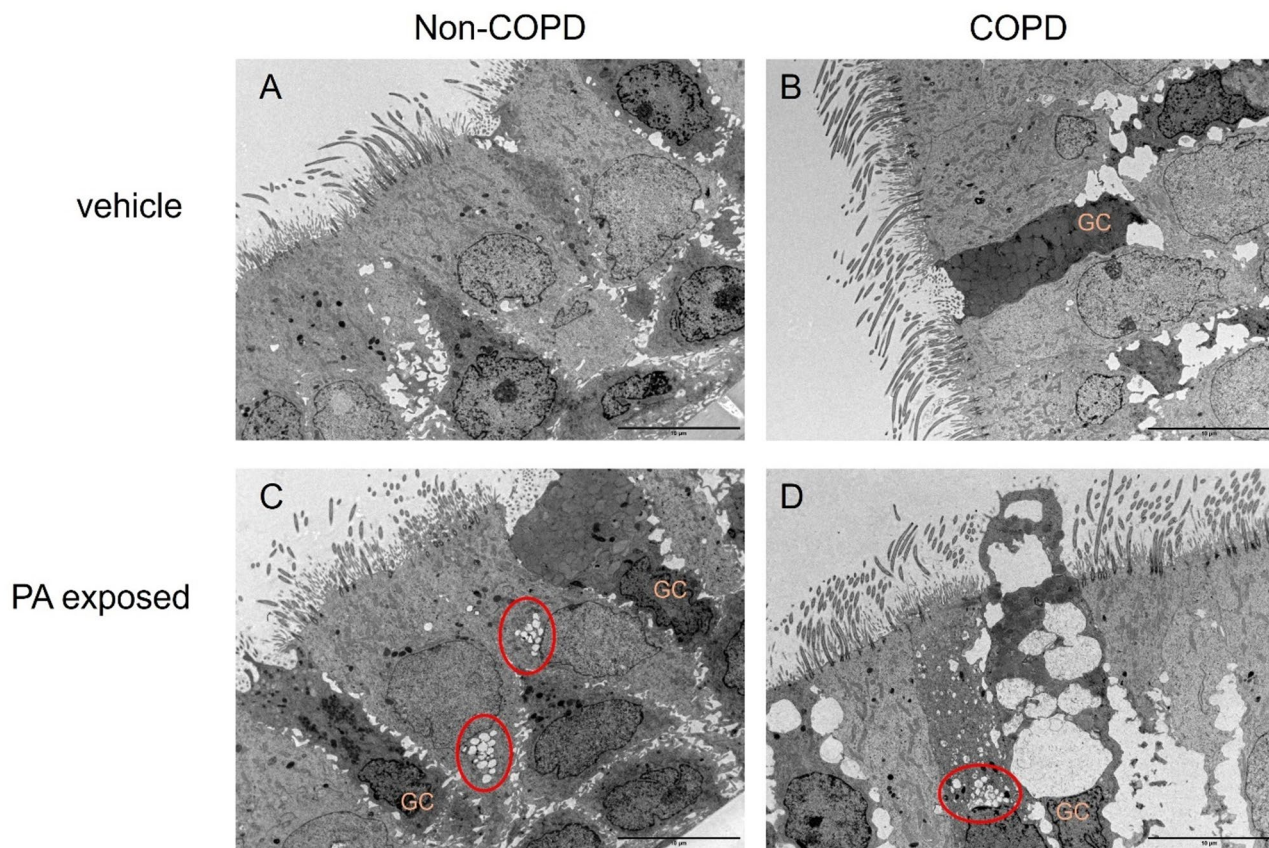


**Fig. 7** Morphological changes in non-COPD/COPD PBEC after polyamide-6.6 (PA) MNP exposure Transmission electron microscopy (TEM) micrographs of differentiated cultures of primary bronchial epithelial cells of non-COPD patients ( $n=2$ ) and COPD patients ( $n=2$ ), exposed to the vehicle control (**A**, **B**, dPBS, 0.05% BSA, 1% 1-propanol) or PA MNPs (**C**, **D**,  $3 \mu\text{g}/\text{cm}^2$ ) for 24 h. Red circles indicate clustered vesicles, visible in ciliated cells after PA exposure. GC: goblet cell. Scale bar represents 10  $\mu\text{m}$

hazard characterization rather than risk assessment, in vitro doses exceeding environmental exposures were applied, to enable identification of potential toxicological mechanisms.

We did not observe significant effects of PVC, PP/Talc or PA MNPs on IL-8 protein secretion or gene expression. This is in contrast with studies using conventional submerged bronchial epithelial cell culture models, that often report induction of pro-inflammatory markers after MNPs exposure. For example, increased inflammatory gene expression was reported in BEAS-2B cells 24 h after exposure with PS, PA or PP/Talc nanoplastics [25, 38]. Unfortunately, studies on the impact of airborne MNPs on bronchial epithelial cell cultures at ALI, which represents a more real-life scenario, are very limited. In line with our findings in PBEC in the current study, in a previous study, we did not observe effects of PA, PP/Talc or PVC MNPs on IL-8 secretion and expression in ALI cultures of bronchial BEAS-2B cells [29]. On the other hand, acute exposure of bronchial Calu-3 ALI cultures via a small droplet to polylactic acid nanoplastics ( $2.5 \mu\text{g}/\text{cm}^2$ ) demonstrated increased levels of Chemokine ligand 20, a chemoattractant for neutrophiles [39]. Using the

same culture model, another study observed increased IL-6 mRNA expression after exposure to PS nanobeads ( $5 \mu\text{g}/\text{cm}^2$ ) [40]. Although being more representative for real life exposure scenario's than their submerged counterparts, these simplistic models lack important physiological features of the bronchial epithelium, including the presence of multiple specialized epithelial cells. In this context, in line with our results, no cytotoxicity, or significant change in IL-8 protein levels was observed after exposure of PBEC to high density polyethylene fragments ( $\pm 40 \mu\text{m}$ ) as well as nylon ( $10 \times 30 \mu\text{m}$ ) fibers ( $\pm 150 \mu\text{g}/\text{cm}^2$ ) [10]. In addition, aerosolized PS spheres (50 nm) also did not impact cytotoxicity (estimated deposition  $3.3 \mu\text{g}/\text{cm}^2$ ) in PBEC [41]. The same study observed increased levels of pro-inflammatory macrophage inflammatory protein-1 alpha, whereas secretion of other cytokines was reduced. IL-8 protein levels were below the limit of quantification. C-X-C motif chemokine 5, another neutrophil attractant, was upregulated in a study exposing PBEC to high doses of dyed polyethylene terephthalate (PET) fibers ( $129.9 \mu\text{g}/\text{cm}^2 \pm 2464 \mu\text{g}/\text{cm}^2$ ) ( $14 \times 45 \mu\text{m}$ ) [42].

Although we observed IL-8 secretion after MNPs exposure in some donors, the response was not statistically significant due to significant inter-donor variation. A high variation in donor response was also observed for other readouts, including antioxidant gene expression and expression of markers for autophagy and apoptosis. Still, a trend could be observed for individual donors. In general, non-COPD donor 2 was most responsive after PA and PVC MNP exposure. In this donor, we observed a strong upregulation of apoptosis marker *BAX*, accompanied with increased expression of antioxidant enzymes. In contrast, high doses of PA significantly downregulated *SOD2* expression in COPD-PBEC, as well as in non-COPD donor 3. These results suggest that the antioxidant response might be impaired in some PBEC, especially those derived from COPD donors. Donor variation previously has been determined to be the most important factor to influence response to nanoparticles [43]. Analysis of different donors in this study allowed us to compare inter-donor variability in response to MNPs, in contrast to conventional studies making use of cell lines that are only derived from a single donor and homogeneous in cell composition. Mucus and surfactant covering the bronchial epithelium, making PBEC physiologically more relevant than submerged or airlifted cell lines [44, 45]. Furthermore, adsorbed phospholipids originating from mucus and surfactants could highly influence particle characteristics including size, protein-corona and agglomeration [46]. Altogether, this highlights the advantage of more advanced ALI cultures for a more accurate prediction of the *in vivo* response to MNPs.

At the level of the bronchial epithelium, it is well established that COPD is characterized by an increased goblet cell population, mucus hypersecretion and decreased amounts of ciliated and club cells [20, 47]. Compared to non-COPD PBEC, only part of these features was recapitulated in COPD PBEC in our study. At baseline, we observed decreased amounts of *Scgb1a1* protein (club cell marker) but no significant differences in gene expression levels of specific epithelial cell markers compared to non-COPD donors. An explanation for this might be the relatively mild disease severity (COPD-II) or the smoking status of the non-COPD donors [48]. For example, goblet cell hyperplasia, marked by increased *MUC5AC* expression, has been convincingly linked to (ex-)smoking status, rather than COPD disease status itself per se [49, 50]. Another observation that has been reported in COPD is decreased barrier integrity of the bronchial epithelium. This characteristic was conserved in the PBEC cultures of COPD patients in our study, as we observed lower TEER levels and a lower expression of genes encoding for tight junction proteins. These results correspond with data from COPD vs. non-COPD PBEC in literature [50]. For some of the non-COPD donors, we

observed increased expression of tight barrier proteins after exposure to MNPs, which might indicate an attempt to re-establish epithelial barrier function. In contrast, PA MNPs decreased the expression of genes encoding tight junction proteins in COPD-PBEC, suggesting these cultures may start to lose the integrity of the epithelial barrier in response to PA MNPs.

In addition to modulation of the expression of tight junction genes, we also observed that MNPs, again in particular PA, altered cell-type-specific gene expression in COPD-PBEC. Indeed, in line with another study that studied the effect of ZnO nanoparticles on COPD-PBEC, we observed reduced expression of ciliated cell marker *FOXJ1* after exposure to PA MNPs [51]. Reduced *FOXJ1* expression has been associated with decreased cilia length [52]. As mucus hypersecretion is observed after several environmental stimuli [53], we hypothesized that MNP-exposure would induce *MUC5AC* expression. This was only true for one non-COPD donor. Remarkably, for COPD PBEC, we observed a decrease in *MUC5AC* expression, after PA or PVC exposure. Since mucus also has a protective role, abnormal *MUC5AC* expression could lead to impaired mucus clearance. Lastly, basal cells were also affected in both non-COPD and COPD-PBEC, which was exemplified by downregulation of *TP63*. As they can differentiate into multiple specific cell types of which the bronchial epithelium consists, basal cells are crucial for the regeneration of airway epithelium after damage. Upon activation by environmental triggers, basal cells transform into fast-proliferating parabasal cells that play a crucial role in tissue repair [54]. The observed decrease in *TP63* mRNA levels in PBEC cultures after PA exposure either suggests a reduced number of bronchial progenitor/stem cells or that PA inhibits the migration and regenerative capacity of these cells.

In an attempt to study uptake of environmentally relevant MNPs, and morphological changes after PA exposure, we performed TEM analysis. Although detection of the unlabeled amorphous MNPs remained difficult with TEM, preliminary data in our study indicated the presence of bright, sometimes clustered intracellular shapes localized in the vicinity of the nucleus. Another study that exposed Calu-3 cells to europium-doped PS nanobeads (45  $\mu\text{g}/\text{cm}^2$ ) revealed the localization of these particles in aggregated intracellular vesicles, often appearing with lamellar bodies [40]. The observed structures in our study could indicate autophagy, especially when they were presented as multilaminar bodies. A recent study observed increased presence of autophagosomes and lysosomes in undifferentiated PBEC submerged exposed to PS microplastics [55]. Another hypothesis is that these structures are lipid vesicles. Abundant amounts of lipids are also present in bronchial cells after viral infection [56]. In addition, engineered metallic nanoparticles have

been shown to induce lipid droplets in cells [57]. The morphological observations in our current pioneering study should be further explored in the future.

Some limitations need to be noted for this study. First of all, it has to be mentioned the non-COPD subjects in this study were not healthy and had a smoking history. Both PBEC from COPD and non-COPD were obtained from resected lung tissue donated by patients undergoing surgery for NSCLC adenocarcinoma. Therefore, it is likely that the observed differences in responses between the two groups stem from the presence or absence of COPD rather than from the predisposition of lung cancer. Secondly, we only studied acute effects of MNPs exposure. This single treatment with MNPs, might underestimate the impact of chronic exposure [39]. Although previous studies in ALI-cultures of Calu-3 cells indicated particle uptake and disruption of tight junctions after 24 h, prolonged exposures (1–2 weeks) resulted in genotoxicity [39]. We applied MNPs on differentiated primary ALI cultures via small droplet application. While this study represents a step forward for the field, which is still highly based on submerged exposures, it might not fully recapitulate inhalation deposition dynamics. Ideally, exposure would have been performed via aerosolization or dry-powder dispensing. However, these approaches require substantial particle quantities, which were limited for the environmentally relevant MNPs used in this study. Furthermore, in this study we made use of sterile, virgin MNPs. MNPs can function as vehicles for bacteria which might lead to increased exacerbation of inflammation in susceptible patients with decreased epithelial barrier function [58]. Lastly, although we evaluated a dose-response in non-COPD PBEC, COPD-PBEC were only exposed to one dose of MNPs (3  $\mu\text{g}/\text{cm}^2$  for PA and 15  $\mu\text{g}/\text{cm}^2$  for PVC and PP/Talc). Also, the number of donors is relatively limited, therefore making it difficult to generalize the observations in this study. To draw firm conclusions on increased vulnerability of bronchial epithelial cells in COPD, our findings should be repeated including more doses and donors. Future studies on pulmonary MNPs toxicity should focus on (pro-longed exposure to) weathered MNPs.

In conclusion, the results of this study suggest that acute exposure to environmentally relevant MNPs does not elicit profound cytotoxicity or inflammation in PBEC but may induce more subtle subtoxic effects at the level of the integrity and cellular composition of the bronchial epithelial layer. PA MNPs appeared to be the most potent of the polymers in eliciting these effects. In addition, preliminary data demonstrates cells from COPD patients may exhibit a slightly increased vulnerability to MNP exposure compared to PBEC derived from non-COPD donors. However, whether or not this implies that COPD patients may be more sensitive to MNP-induced toxicity

or that MNP may play a role in development or progression of the disease remains to be established. Improving our understanding of the cellular effects of MNPs on both diseased and non-diseased bronchial epithelial cells represents an important step toward elucidating potential risks of MNPs on respiratory health.

#### Abbreviations

ACTB	Beta-actin
ALI	Air-liquid interface
B2M	Beta-2 microglobulin
BALF	Bronchoalveolar lavage fluid
BAX	Bcl-2 Associated X, Apoptosis Regulator
BSA	Bovine serum albumin
COPD	Chronic obstructive pulmonary disease
CLDN3	Claudin 3
CLDN4	CLAUDIN 4
CuO	Copper(II) oxide
CXCL8	C-X-C motif chemokine ligand 8
CYPA	Cyclophilin A
D <sub>N</sub>	Medium number-based size
D <sub>V</sub>	Median volume-based size
dPBS	Dulbecco's Phosphate Buffered Saline
FEV <sub>1</sub>	forced expiratory volume in the first second
FOXJ1	Forkhead box J1
FVC	Forced vital capacity
GABARAPL1	GABA Type A Receptor Associated Protein Like 1
IL-6	Interleukin-6
IL-8	Interleukin-8
KRT5	Keratin 5
LAL	Limulus Amebocyte Lysate
LDH	Lactate dehydrogenase
MPTC	Maastricht Pathology Tissue Collection
MQ	MilliQ-water
MNPs	Microplastics and nanoplastics
MUC5AC	Mucin-5AC
NSCLC	Non-Small Cell Lung Carcinoma
OCLN	Occludin
PA	Polyamide-6,6
PBEC	Primary bronchial epithelial cells
PET	Polyethylene terephthalate
PP	Polypropylene
PS	Polystyrene
PVC	Polyvinylchloride
ROS	Reactive oxygen species
RPL13A	Ribosomal protein L13A
SCGB1A1	Secretoglobin Family 1 A Member 1
SOD1	Superoxide Dismutase 1
SOD2	Superoxide Dismutase 2
SQSTM1	Sequestosome 1
TEER	Transepithelial electrical resistance
TEM	Transmission electron microscopy
TNF- $\alpha$	Tumor Necrosis Factor Alpha
TP63	Tumor protein P63
qPCR	Polymerase chain reaction
(ZO)-1	ZONULA occludens-1

#### Supplementary Information

The online version contains supplementary material available at <https://doi.org/10.1186/s43591-025-00166-1>.

- Supplementary Material 1
- Supplementary Material 2
- Supplementary Material 3
- Supplementary Material 4
- Supplementary Material 5

## Acknowledgements

The authors would like to thank the Primary Lung Culture Facility (PLUC; Maastricht University Medical Center+, The Netherlands) for providing advice. We acknowledge Carmen López Iglesias and Willine Van de Wetering (Microscopy CORE Lab, Maastricht University) for TEM sample preparation, fruitful discussions and technical advice. In addition, we would like to thank Christy Tulen, for performing the characterization study on ciliary beating/deposition. Lastly, we would like to thank Maria Kloukinioti (Netherlands Organization for Applied Scientific Research, TNO) for her assistance with the LAL assay.

## Author contributions

I.F.G: Writing – review & editing, Writing – original draft, Methodology, Conceptualization, Investigation, Visualization, Formal analysis. P.L.: Investigation. M.J.D: Investigation. E.W: Investigation. P.J.J.J: Investigation. F.G.A.J.B: Investigation. K.S.: Writing – review & editing. I.M.K: Supervision, Conceptualization. F.J.S: Supervision, Writing – review & editing, Project administration. A.H.R: Writing – review & editing, Supervision, Conceptualization, Project administration. All authors read and approved the final manuscript.

## Funding

This work is part of the MOMENTUM and MOMENTUM2.0 projects. The MOMENTUM project was made possible by ZonMw Programme Microplastics and Health, and Health-Holland, Top Sector Life Sciences & Health (project number 458001101). The MOMENTUM2.0 is funded by ZonMw Programme Microplastics and Health (project number 4580012310002).

## Data availability

Data are publicly available on YODA, a data repository built and maintained by Utrecht University. Data can be found via the following link: <https://doi.org/10.24416/UU01-RZ2DH0>. Data can be used under the Deed - Attribution 4.0 International - Creative Commons license, please refer to the original manuscript when using the data.

## Declarations

### Competing interests

The authors declare no competing interests.

Received: 18 August 2025 / Accepted: 4 December 2025

Published online: 30 December 2025

## References

1. Neira M, Fones G. Air pollution: tackling a critical driver of the global NCD crisis Available from: <https://www.who.int/news-room/commentaries/detail/air-pollution--tackling-a-critical-driver-of-the-global-ncd-crisis>: World Health Organization; 2025.
2. Kau D, Materić D, Holzinger R, Baumann-Stanzer K, Schauer G, Kasper-Giebl A. Fine micro-and nanoplastics concentrations in particulate matter samples from the high alpine site Sonnblick, Austria. *Chemosphere*. 2024;352:141410.
3. Eberhard T, Casillas G, Zarus GM, Barr DB. Systematic review of microplastics and nanoplastics in indoor and outdoor air: identifying a framework and data needs for quantifying human inhalation exposures. *J Expo Sci Environ Epidemiol*. 2024;34(2):185–96.
4. Mohamed Nor NH, Kooi M, Diepens NJ, Koelmans AA. Lifetime accumulation of microplastic in children and adults. *Environ Sci Technol*. 2021;55(8):5084–96.
5. Zhao X, Zhou Y, Liang C, Song J, Yu S, Liao G, et al. Airborne microplastics: Occurrence, sources, fate, risks and mitigation. *Sci Total Environ*. 2023;858:159943.
6. Huang X, Saha SC, Saha G, Francis I, Luo Z. Transport and deposition of microplastics and nanoplastics in the human respiratory tract. *Environ Adv*. 2024;16:100525.
7. Jenner LC, Rotchell JM, Bennett RT, Cowen M, Tentzeris V, Sadofsky LR. Detection of microplastics in human lung tissue using  $\mu$ FTIR spectroscopy. *Sci Total Environ*. 2022;831:154907.
8. Uogintė I, Vailionytė A, Skapas M, Bolanos D, Bagurskiene E, Gruslys V, et al. New evidence of the presence of micro-and nanoplastic particles in bronchioalveolar lavage samples of clinical trial subjects. *Heliyon*. 2023;9(9).
9. Baeza-Martínez C, Olmos S, González-Pleiter M, López-Castellanos J, García-Pachón E, Masiá-Canuto M, et al. First evidence of microplastics isolated in European citizens' lower airway. *J Hazard Mater*. 2022;438:129439.
10. Donkers JM, Höppener EM, Grigoriev I, Will L, Melgert BN, van der Zaan B, et al. Advanced epithelial lung and gut barrier models demonstrate passage of microplastic particles. *Microplastics Nanoplastics*. 2022;2(1):6.
11. Brits M, Van Velzen MJ, Sefiloglu FÖ, Scibetta L, Groenewoud Q, García-Vallejo JJ, et al. Quantitation of micro and nanoplastics in human blood by pyrolysis-gas chromatography–mass spectrometry. *Microplastics Nanoplastics*. 2024;4(1):12.
12. Wang Z, Lin J, Liang L, Huang F, Yao X, Peng K, et al. Global, regional, and National burden of chronic obstructive pulmonary disease and its attributable risk factors from 1990 to 2021: an analysis for the global burden of disease study 2021. *Respir Res*. 2025;26(1):2.
13. Vasse GF, Melgert BN. Microplastic and plastic pollution: impact on respiratory disease and health. *Eur Respiratory Rev*. 2024;33(172).
14. Prata JC. Airborne microplastics: consequences to human health? *Environ Pollut*. 2018;234:115–26.
15. Huang S, Huang X, Bi R, Guo Q, Yu X, Zeng Q, et al. Detection and analysis of microplastics in human sputum. *Environ Sci Technol*. 2022;56(4):2476–86.
16. Aghapour M, Raee P, Moghaddam SJ, Hiemstra PS, Heijink IH. Airway epithelial barrier dysfunction in chronic obstructive pulmonary disease: role of cigarette smoke exposure. *Am J Respir Crit Care Med*. 2018;58(2):157–69.
17. Carlier FM, de Fays C, Pilette C. Epithelial barrier dysfunction in chronic respiratory diseases. *Front Physiol*. 2021;12:691227.
18. Kim V, Oros M, Durra H, Kelsen S, Aksoy M, Cornwell WD, et al. Chronic bronchitis and current smoking are associated with more goblet cells in moderate to severe COPD and smokers without airflow obstruction. *PLoS ONE*. 2015;10(2):e0116108.
19. Yaghi A, Zaman A, Cox G, Dolovich MB. Ciliary beating is depressed in nasal cilia from chronic obstructive pulmonary disease subjects. *Respir Med*. 2012;106(8):1139–47.
20. Heijink IH, Noordhoek JA, Timens W, van Oosterhout AJ, Postma DS. Abnormalities in airway epithelial junction formation in chronic obstructive pulmonary disease. *Am J Respir Crit Care Med*. 2014;189(11):1439–42.
21. Wang T, Dong Y, Fang L, Zhou H. Patterns and underlying mechanisms of airway epithelial cell death in COPD. *COPD: J Chronic Obstr Pulm Dis*. 2025;22(1):2542153.
22. Demedts IK, Demoor T, Bracke KR, Joos GF, Brusselle GG. Role of apoptosis in the pathogenesis of COPD and pulmonary emphysema. *Respir Res*. 2006;7(1):53.
23. Gou Z, Wu H, Li S, Liu Z, Zhang Y. Airborne micro-and nanoplastics: emerging causes of respiratory diseases. *Part Fibre Toxicol*. 2024;21(1):1–22.
24. Yang S, Zhang T, Ge Y, Yin L, Pu Y, Liang G. Inhalation exposure to polystyrene nanoplastics induces chronic obstructive pulmonary disease-like lung injury in mice through multi-dimensional assessment. *Environ Pollut*. 2024;347:123633.
25. Gosselink I, Leonhardt P, Höppener E, Smelt R, Drittij M, Davigo M, et al. Size- and polymer-dependent toxicity of amorphous environmentally relevant micro- and nanoplastics in human bronchial epithelial cells. *Microplastics Nanoplastics*. 2025;5(1):1–17.
26. Wright S, Cassee FR, Erdely A, Campen MJ. Micro-and nanoplastics concepts for particle and fibre toxicologists. *Part Fibre Toxicol*. 2024;21(1):18.
27. Mertens TC, Karmouty-Quintana H, Taube C, Hiemstra PS. Use of airway epithelial cell culture to unravel the pathogenesis and study treatment in obstructive airway diseases. *Pulm Pharmacol Ther*. 2017;45:101–13.
28. Parker LA, Höppener EM, van Amelrooij EF, Henke S, Kooter IM, Grigoradi K, et al. Protocol for the production of micro- and nanoplastic test materials. *Microplastics Nanoplastics*. 2023;3(1):10.
29. Gosselink IF, van Schooten FJ, Drittij MJ, Höppener EM, Leonhardt P, Moschini E, et al. Assessing toxicity of amorphous nanoplastics in airway- and lung epithelial cells using air-liquid interface models. *Chemosphere*. 2024;368:143702.
30. Sample Passports MOMENTUM. Test Materials. [Internet]. 2024.
31. Van Wetering S, van der Linden AC, van Sterkenburg MA, de Boer WI, Kuijpers AL, Schalkwijk J, et al. Regulation of SLPI and Elafin release from bronchial epithelial cells by neutrophil defensins. *Am J Physiology-Lung Cell Mol Physiol*. 2000;278(1):L51–8.
32. Tulen CB, Duistermaat E, Cremers JW, Klerk WN, Fokkens PH, Weibolt N, et al. Smoking-associated exposure of human primary bronchial epithelial cells

to aldehydes: impact on molecular mechanisms controlling mitochondrial content and function. *Cells*. 2022;11(21):3481.

33. Vandesompele J, De Preter K, Pattyn F, Poppe B, Van Roy N, De Paepe A, et al. Accurate normalization of real-time quantitative RT-PCR data by geometric averaging of multiple internal control genes. *Genome Biol*. 2002;3(7):research00341.
34. Liu S, Yao S, Yang H, Liu S, Wang Y. Autophagy. Regulator of cell death. *Cell Death Dis*. 2023;14(10):648.
35. Pease JE, Sabroe I. The role of interleukin-8 and its receptors in inflammatory lung disease: implications for therapy. *Am J Respir Med*. 2002;1(1):19–25.
36. Kirkham PA, Barnes PJ. Oxidative stress in COPD. *Chest*. 2013;144(1):266–73.
37. Mercer RR, Russell ML, Roggli VL, Crapo JD. Cell number and distribution in human and rat airways. *Am J Respir Cell Mol Biol*. 1994;10(6):613–24.
38. Yang S, Cheng Y, Chen Z, Liu T, Yin L, Pu Y, et al. In vitro evaluation of nanoplastics using human lung epithelial cells, microarray analysis and co-culture model. *Ecotoxicol Environ Saf*. 2021;226:112837.
39. García-Rodríguez A, Gutiérrez J, Villacorta A, Arranz JA, Romero-Andrade I, Lacoma A, et al. Polyactic acid nanoplastics (PLA-NPLs) induce adverse effects on an *in vitro* model of the human lung epithelium: the Calu-3 air-liquid interface (ALI) barrier. *J Hazard Mater*. 2024;475:134900.
40. Michelini S, Mawas S, Kurešepi E, Barbero F, Šimunović K, Miremont D, et al. Pulmonary hazards of nanoplastic particles: a study using polystyrene in *in vitro* models of the alveolar and bronchial epithelium. *J Nanobiotechnol*. 2025;23(1):388.
41. Breidenbach JD, French BW, Shrestha U, Adya ZK, Wooten RM, Fribley AM, et al. Acute exposure to aerosolized nanoplastics modulates Redox-Linked immune responses in human airway epithelium. *Antioxidants*. 2025;14(4):424.
42. O'Connor A, Santeli AV, Shankar SN, Shirkhani A, Baker TR, Wu C-Y, et al. Toxicity of microplastic fibers containing Azobenzene disperse dyes to human lung epithelial cells cultured at an air-liquid interface. *J Hazard Mater*. 2024;480:136280.
43. Kooter IM, Gröllers-Mulderij M, Duistermaat E, Kuper F, Schoen ED. Factors of concern in a human 3D cellular airway model exposed to aerosols of nanoparticles. *Toxicol in Vitro*. 2017;44:339–48.
44. Busch M, Brouwer H, Aalderink G, Bredeck G, Kämpfer AA, Schins RP, et al. Investigating nanoplastics toxicity using advanced stem cell-based intestinal and lung *in vitro* models. *Front Toxicol*. 2023;5:1112212.
45. Silva S, Bicker J, Falcão A, Fortuna A. Air-liquid interface (ALI) impact on different respiratory cell cultures. *Eur J Pharm Biopharm*. 2023;184:62–82.
46. Shi W, Cao Y, Chai X, Zhao Q, Geng Y, Liu D, et al. Potential health risks of the interaction of nanoplastics and lung surfactant. *J Hazard Mater*. 2022;429:128109.
47. Laacho-Contreras ME, Polverino F, Gupta K, Taylor KL, Kelly E, Pinto-Plata V, et al. Protective role for club cell secretory protein-16 (CC16) in the development of COPD. *Eur Respir J*. 2015;45(6):1544–56.
48. Nwozor KO, Hackett T-L, Chen Q, Yang CX, Aguilar Lozano SP, Zheng X, et al. Effect of age, COPD severity, and cigarette smoke exposure on bronchial epithelial barrier function. *Am J Physiology-Lung Cell Mol Physiol*. 2025;328(5):L724–37.
49. Lappere TS, Sont JK, van Schadewijk A, Gosman MM, Postma DS, Bajema IM, et al. Smoking cessation and bronchial epithelial remodelling in COPD: a cross-sectional study. *Respir Res*. 2007;8:1–9.
50. Carlier FM, Detry B, Lecocq M, Collin AM, Planté-Bordeneuve T, Gérard L, et al. The memory of airway epithelium damage in smokers and COPD patients. *Life Sci Alliance*. 2024;7(3).
51. Stoleriu MG, Ansari M, Strunz M, Schamberger A, Heydarian M, Ding Y, et al. COPD basal cells are primed towards secretory to multiciliated cell imbalance driving increased resilience to environmental stressors. *Thorax*. 2024;79(6):524–37.
52. Brekman A, Walters MS, Tilley AE, Crystal RG. FOXJ1 prevents cilia growth Inhibition by cigarette smoke in human airway epithelium *in vitro*. *Am J Respir Cell Mol Biol*. 2014;51(5):688–700.
53. Memon TA, Nguyen ND, Burrell KL, Scott AF, Almestica-Roberts M, Rapp E, et al. Wood smoke particles stimulate MUC5AC overproduction by human bronchial epithelial cells through TRPA1 and EGFR signaling. *Toxicol Sci*. 2020;174(2):278–90.
54. Ganesan S, Sajjan US. Repair and remodeling of airway epithelium after injury in chronic obstructive pulmonary disease. *Curr Respiratory Care Rep*. 2013;2:145–54.
55. Wei YY, Ting CT, Wei ZD, Ying Z, Fang L, Chuan DY, et al. Microplastics exacerbate ferroptosis via mitochondrial reactive oxygen species-mediated autophagy in chronic obstructive pulmonary disease. *Autophagy*. 2025;21(8):1717–43.
56. Nardacci R, Colavita F, Castilletti C, Lapa D, Matusali G, Meschi S, et al. Evidences for lipid involvement in SARS-CoV-2 cytopathogenesis. *Cell Death Dis*. 2021;12(3):263.
57. Khatchadourian A, Maysinger D. Lipid droplets: their role in Nanoparticle-Induced oxidative stress. *Mol Pharm*. 2009;6(4):1125–37.
58. Sethi S, Murphy TF. Infection in the pathogenesis and course of chronic obstructive pulmonary disease. *N Engl J Med*. 2008;359(22):2355–65.

## Publisher's note

Springer Nature remains neutral with regard to jurisdictional claims in published maps and institutional affiliations.